A Simple Quasi-2D Numerical Model of a Thermogage Furnace

K. Chahine[1, 3], M. Ballico[1], J. Reizes[2] and J. Madadnia[2]

[1] National Measurement Institute, NMIA, Australia.

[2] University of Technology, Sydney.

[3] E-mail: Khaled.Chahine@nmi.gov.au

ABSTRACT

A simple quasi 2-D model for the temperature distribution in a graphite tube furnace is presented. The model is used to estimate the temperature gradients in the furnace at temperatures above which contact sensors can be used, and to assist in the redesign of the furnace heater element to improve the temperature gradients.

The Thermogage graphite tube furnace is commonly used in many NMIs as a blackbody source for radiation thermometer calibration and as a spectral irradiance standard. Although the design is robust, easy to operate and can change temperature rapidly, it is limited by its effective emissivity of typically 99.5 to 99.8 %. At NMIA, the temperature gradient along the tube is assessed using thermocouples up to about 1500 °C, and the blackbody emissivity is calculated from this. However, at higher operating temperatures (up to 2900 °C), it is impractical to measure the gradient, and we propose to numerically model the temperature distributions used to calculate emissivity. In another paper at this conference, the model is used to design an optimised heater tube with improved temperature gradients.

In the model presented here, the 2-D temperature distribution is simplified to separate the axial and radial temperature distributions within the heater tube and the surrounding insulation. Literature data for temperature dependence of the electrical and thermal conductivity of the graphite tube was coupled to models for the thermal conductivity of the felt insulation, particularly including the effects of allowing for a gas mixture in the insulation.

Experimental measurements of the temperature profile up to 1500 °C and radial heat fluxes up to 2200 °C were compared to the theoretical predictions of the model and good agreement was obtained.

KEY WORDS: ATJ graphite; blackbody; graphite felt; numerical model; Thermogage.

1. INTRODUCTION

A 48 kW Thermogage blackbody furnace is used as a spectrally calculable source of radiation for standard spectral irradiance and for the temperature calibrations of pyrometers up to 3000 °C. At NMIA, the increasingly stringent uncertainty requirements from industry necessitate improvement of the temperature uncertainty associated with using this blackbody. Presently, this uncertainty is approximately 2 °C at 2000 °C, and mainly due to the emissivity of the blackbody as calculated from its temperature distribution [1]. Other blackbody designs use a profiled graphite tube to improve the temperature distribution, however the heat transfer mechanisms change significantly over the range 1000 to 3000 °C, and it is difficult to "tune" this profile to achieve the desired effect at all temperatures. Further, modifications to the furnace must ensure that the tube current and voltage and silica tube temperature remain within design constraints. To facilitate the tube redesign, a simple quasi 2-D model has been developed to numerically simulate the graphite tube inner temperature profile. This software will be used to optimise the design of the graphite tube in order to obtain good temperature uniformity over a wide temperature range.

2. THERMOGAGE FURNACE

The Thermogage blackbody furnace (Fig. 1) consists of an ATJ graphite tube surrounded by insulating material, which consists of graphite felt purged with an inert gas wrapped with two layers of graphite foils and inserted into a silica tube. For some years at NMIA we have been using graphite tubes, 289 mm long with 31.8 mm OD and 3.2 mm wall thickness, machined from rods of ATJ grade graphite. In this paper we consider one of the NMIA tubes which has been machined with a region of lower wall thickness in an attempt to improve the temperature uniformity. The graphite felt, from Morgan, has a density of 90 $kg.m^{-3}$ with 22 μm-diameter fibres. The tube and its insulation are surrounded by a water-cooled jacket. The water-jacket function is to prevent accidental contact with the hot surface of the silica tube and to capture the radial heat flux where it is measured calorimetrically. The ends of the tube are clamped by graphite-composite rings, which are in turn clamped to water-cooled copper rings. During operation, the graphite tube and graphite-composite rings are ohmically heated by a voltage applied across the copper rings. This electrical power is dissipated by (i) conduction along the graphite tube, (ii) radiation from the middle of the tube and (iii) radially through the insulation.

As the temperature gradient in the insulation surrounding the tube is mostly radial, whilst that in the graphite tube itself is mostly axial, the 2-D heat flows in the system were separated into 1-D heat transfer problems which can be solved separately by the finite elements method and then coupled (Fig. 2). The graphite-composite rings pose a special challenge as they have a complex 3-D structure and are affected by contact resistances which are difficult to determine. They are modelled as lumped electrical and thermal resistances which are determined experimentally.

2.1. Graphite Tube

The graphite tube is modelled as a 1-D heat transfer problem. NMIA manufactures its own tubes from ATJ graphite. We adopt the literature values for the temperature dependent electrical [2] and thermal [2, 3] conductivities. As the grain orientations in our ATJ samples appeared random, we adopted the anisotropic value $\frac{2}{3}k_{\perp} + \frac{1}{3}k_{\parallel}$ (Fig. 3). The tube was modelled as $m \approx 50$ very short "tube elements" of varying diameter and thickness through which a fixed current flows, generating heat (I^2R) within each element. The element in the centre of the tube is considered as the "tube septum", and is a special element considered as a disk. We model three heat fluxes from each element:

1. Thermal conduction to adjacent elements.
2. Thermal radiation between the element and other elements in the tube (the "cold" end and the "septum" are special here). This entails calculation of the order of m^2 radiant transfer view factors, given in [4]. As the emissivity of graphite is assumed to be approximately 0.8, for simplicity only direct radiative transfer is considered: second reflections are ignored.

3. Radial heat flux from the outer surface of each element to ambient. This is considered as a thermal resistor whose resistance (considered later) is dependent on the temperature of the "hot" end.

2.2. Radial Thermal Resistance, $R_{Radial}(T)$

As the radial heat flux dominates the central, uniform temperature region of the tube in which we are most interested, this is the key to the model. We consider this as a purely 1-D radial heat transfer problem (i.e. assume axial uniformity). As the insulation layer is thin (15 mm) compared to the scale length of the axial temperature gradients, this is a reasonable approximation. This problem is solved by finite elements (Fig. 2) in the radial direction. Three regions thermally in series are considered:

1. R_{Felt} : The graphite felt is modelled as n ≈ 10 annular rings. The temperature-dependent thermal conductivity was extensively investigated in [7], resulting in a simple model giving the conductivity as a function of felt density (given by solid fraction f), fibre radius (r) and filling gas conductivity k_{gc}.

$$k_f(T) = \frac{k_{gc}(T) + C_{fr}\sigma \frac{r}{f} T^3}{1-f} + 3.5\times10^{-4} k_s(T)$$

   Where σ is the Stefan-Boltzmann constant, k_s is the thermal conductivity of the graphite fibres, and C_{fr} is a radiation constant with values determined from the literature to be around 15.0. Fig. 3 shows the computed thermal conductivity for He and N_2 used as shield gases. For other gas mixtures the molar fraction weighted-average gas conductivity is used. Note that at low temperatures, using He significantly increases the conductivity from the N_2 value. This was found to be important for later work using the gas mix to "tune" the furnace gradient.

2. R_{foils} : The graphite felt is surrounded by several layers of graphite foil, which act as radiation shields. The conduction from the felt to the foil, between the layers of foil, from the foils to the silica tube holding the assembly, and through the silica tube are calculated from the thermal conductivity of the inert gas mixture and the radiation, assuming an emissivity of 0.8 for graphite and 1.0 for the silica. As the gaps between

the layers (assumed to be 0.5 mm) are small, convection is neglected. Overall, the contribution from this resistance is very small.

3. $R_{Water\ Jacket}$: The thermal resistance across the 10 mm air gap between the silica tube and the water jacket is modelled as two concentric cylinders with the heat transfer between them occurring by free convection [5, p 564] and by radiation [6, p 299].

This heat transfer problem was solved using the iterative over-relaxation method on $n+2$ finite elements in an EXCEL spreadsheet. It was solved for a number of temperatures of the "hot" end, to give a simple polynomial for the temperature dependence of the total radial thermal resistance $R_{Radial}(T)$. The dominant thermal resistance is that of the graphite felt.

2.3. Tube End Thermal Resistance, R_{cc}

The two ends of the graphite tube are held in short graphite-composite (CC) sleeves, which contribute significant electrical heating and have complex 3-D geometry contact resistances making them difficult to model numerically. We note that whatever design for the graphite tube or insulation system was used, this "sleeve" section would remain the same. We therefore adopt an empirical approach and consider these end components as lumped elements whose electrical and thermal resistances are experimentally determined as a function of the temperature of the "hot" end of the CC-sleeve. The electrical resistance is determined by measuring the voltage drop between the copper electrode and the end of the ATJ graphite tube, and the current through the tube with a current transformer around the copper electrode. The thermal resistance R_{cc} is determined by measuring the temperature of the end of the ATJ graphite tube and the total heat flux passing through the CC-sleeve.

$$T_1 - T_{amb} = R_{cc}(T_1)\left[kA\frac{dT}{dx} + \frac{IV_{elec}}{2}\right]$$

This has two parts, the heat flux $kA\frac{dT}{dx}$ coming from the end of the ATJ tube and the electric power IV_{elec} heating it. The factor of 2 in the ohmic heating arises because the power is assumed to be deposited evenly throughout the CC-sleeve, not at the "hot" end only. These factors are plotted in Fig. 4.

3. EXPERIMENTAL APPARATUS

The water cooling jacket enclosing the silica tube containing the insulation and graphite tube was used as a calorimeter to measure the total heat flux leaving the tube radially. The flow rate of cooling water was measured with a calibrated domestic water meter, and the temperature drop (typically a few °C) between inlet and outlet temperatures was measured with an accuracy estimated at 0.02 °C with a differential type-T thermocouple. The calorimeter was estimated to capture 80-90 % of the radial flux, the remainder escaping by convection from the ends of the water jacket. The temperature of the silica tube was measured with a type-K thermocouple, to allow checking the estimated value for the silica-tube to water jacket air-gap thermal resistance. The voltage across the electrodes and the current through the tube were also measured. As the tube current supply was a simple AC thyristor system providing truncated 50 Hz AC, measurements were made by an RMS integrating voltmeter with tested high frequency response.

Accurately measuring the axial temperature profile within the graphite tube is difficult because the strong axial temperature gradients can cause significant conduction errors. In [4] the effectiveness of several different designs of thermocouples and of a specially-developed optical fibre technique were assessed to determine suitable techniques for measuring the temperature profile. For the work here, it was measured using an alumina-sheathed type-R thermocouple with a few cm of the thermocouple wire formed into a "ring" against the wall of the graphite tube to avoid systematic errors caused by conduction down the thermocouple. Thermocouple measurements are made at 10 mm intervals along the tube by a translation stage, positioned with a precision better than 1 mm.

4. RESULTS & DISCUSSION

Fig. 5 shows the measured temperature profiles in the tube for He and N_2 shielding gases at both 1000 and 1500 °C. The region up to about 70 mm is relatively uniform in temperature, falling rapidly to about 400 °C at the junction of the CC-sleeve and graphite tube, and the model predicts this satisfactorily for the 1000 °C case. In the 1500 °C case the measured temperatures are systematically higher than those modelled. However, in both cases, the predicted change in profile with change from the lower conductance N_2 shield gas to the higher conductance He gas is in reasonable agreement. It is proposed to use this shield gas effect as a technique to tune the temperature profile of a given rod to achieve uniformity over a wider range of operating temperatures.

The increase in temperature in the region around 60 mm, arising from the N_2 to He change can be understood to result from the higher radial heat flux decreasing the relative effect of axial conduction along the rod. At higher temperatures the thermal conductivity of the graphite decreases, whilst that of the felt increases, leading to a similar effect (consider the limiting cases of zero axial heat flux, when axial uniformity may be expected, or zero radial heat flux, when a parabolic distribution may be expected). In this tube design we can see that the "thin wall" section suitable to "peak up" the gradient at 1000 °C produces too large an effect at 1500 °C.

Fig. 6 shows the measured and calculated radial heat fluxes from the graphite felt insulation. The data are in good agreement with the model at 1000 °C and increase in a similar way with increasing tube operating temperature, however the difference between the measured data and the modelled data increases to 30 % at 2200 °C. On the other hand, the predicted change in radial heat flux with change from N_2 to He shield gas is quite consistent with the measured data. Fig. 7 shows the temperature of the silica tube holding the shield gas around the graphite felt. As with the heat flux data the agreement is good at lower temperatures and diverges at higher temperatures. Again the measured difference between N_2 and He is close to that predicted.

Part of the discrepancy in radial heat flux and consequent silica tube temperature may be due to the 10-20 % convective heat loss which presently escapes from the sides of the cooling jacket; for free convection the fraction of loss may be expected to increase with temperature as observed here. Also, upon disassembly of this tube, which had also been used up to 2900 °C, the graphite felt was observed to be loaded with graphite powder, evaporated from the rod and condensed into the lower temperature regions of the felt. This would lead to a decrease in its conductivity (dominated by the thermal photon mean free path), and consequent decrease in observed heat flux and silica tube temperature.

5. CONCLUSIONS

A simple quasi 2-D numerical model was developed with the aim of creating a simple tool for optimisation of the temperature profile of NMIA's Thermogage graphite tube furnace. The model takes as input (a) physical dimensions, (b) literature values for the thermal conductivity of graphite, N_2 and He, (c) the density and fibre diameter of the graphite felt insulation, (d) the applied heating current and (e) empirically determined values for the electrical and thermal conductivity of the CC-sleeve. It computes the tube temperature profile, heat fluxes and tube voltage. Experimentally measured heat fluxes and temperature profiles at 1000 and 1500 °C using both He and N_2 shielding gases are in reasonable agreement with the model calculations. The main limitation of this model is the need to use an empirical model for the thermal conductance of the CC-sleeves. The uncertainty in knowledge of the thermal conductivity of the graphite and felt insulation, especially after heating to high temperatures, also reduces the accuracy of the model. The model has been found useful in developing strategies for the optimisation of this type of furnace, such as changing the inert shield gas; however, it requires some additional refinement before it can be used for accurate quantitative predictions of the temperature profiles.

REFERENCES

1. M. Ballico, *Metrologia* **37**:4 (2000).

2. Y. S. Touloukian, *Thermal Conductivity: Nonmetallic solids.* New York, IFI/Plenum (1970).

3. C. L. Mantell, Carbon and graphite handbook, New York, Interscience Publishers (1968).

4. K. Chahine, M. Ballico, J. Reizes, J. Madadnia, *Temperature Profile Measurement of a Graphite Tube Using Optical Fibre and Platinum Thermocouples*, Metrological Society of Australia Conference, Canberra (2005).

5. F. P. Incropera, D. P. Dewitt, *Fundamentals of Heat and Mass Transfer*, New York, Wiley (2002).

6. R. Siegell, J. R. Howell, *Thermal Radiation Heat Transfer*, London, Taylor & Francis (2002).

7. K. Chahine, M. Ballico, J. Reizes, J. Madadnia, *Thermal Conductivity of Graphite Felt at High Temperatures*, The 8th Australasia Heat and Mass Transfer Conference, Perth (2005).

FIGURE CAPTIONS

Fig. 1. Schematic diagram of the NMI 48 kW Thermogage graphite furnace.

Fig. 2. Equivalent thermal circuit diagram of the ATJ graphite furnace tube.

Fig. 3. Graph of the thermal conductivities of ATJ graphite in the parallel and perpendicular direction and their average, and that of the Morgan graphite felt mixed with nitrogen and helium versus the absolute temperatures.

Fig. 4. Plot of the graphite-composite electrical and thermal heat fluxes versus the average of the ambient and the first node (T_1) temperatures.

Fig. 5. Comparison of the measured temperature profile with the predictions of the model at operating temperatures of 1000 and 1500 °C with the graphite felt purged in nitrogen and helium.

Fig. 6. Comparison of the measured radial heat fluxes with the modelled ones at operating temperatures ranging from 1000 to 2200 °C.

Fig. 7. Comparison of the measured silica tube middle temperatures with the model predictions at operating temperatures ranging from 1000 to 2200 °C.

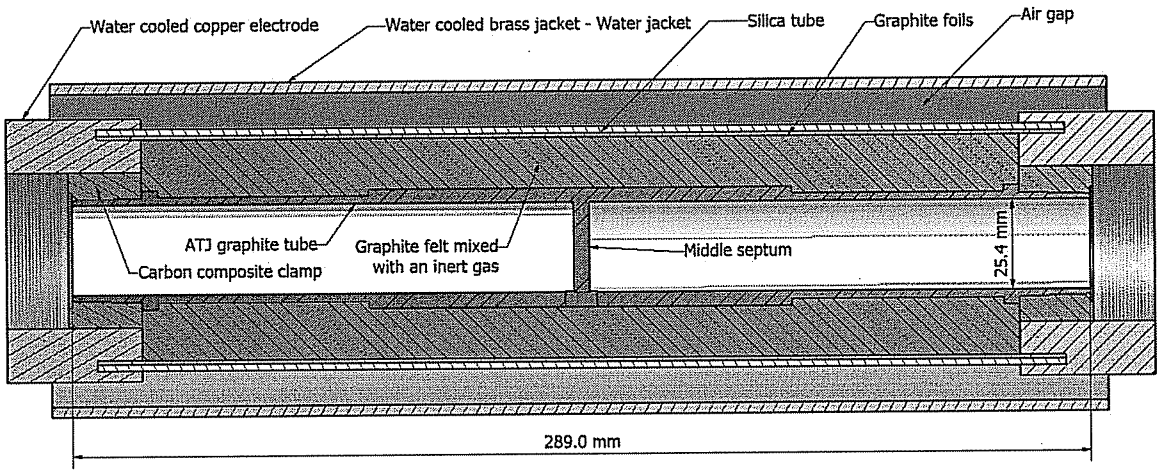
Water cooled copper electrode
Water cooled brass jacket - Water jacket
Silica tube
Graphite foils
Air gap
ATJ graphite tube
Carbon composite clamp
Graphite felt mixed with an inert gas
Middle septum
25.4 mm
289.0 mm

Fig. 1

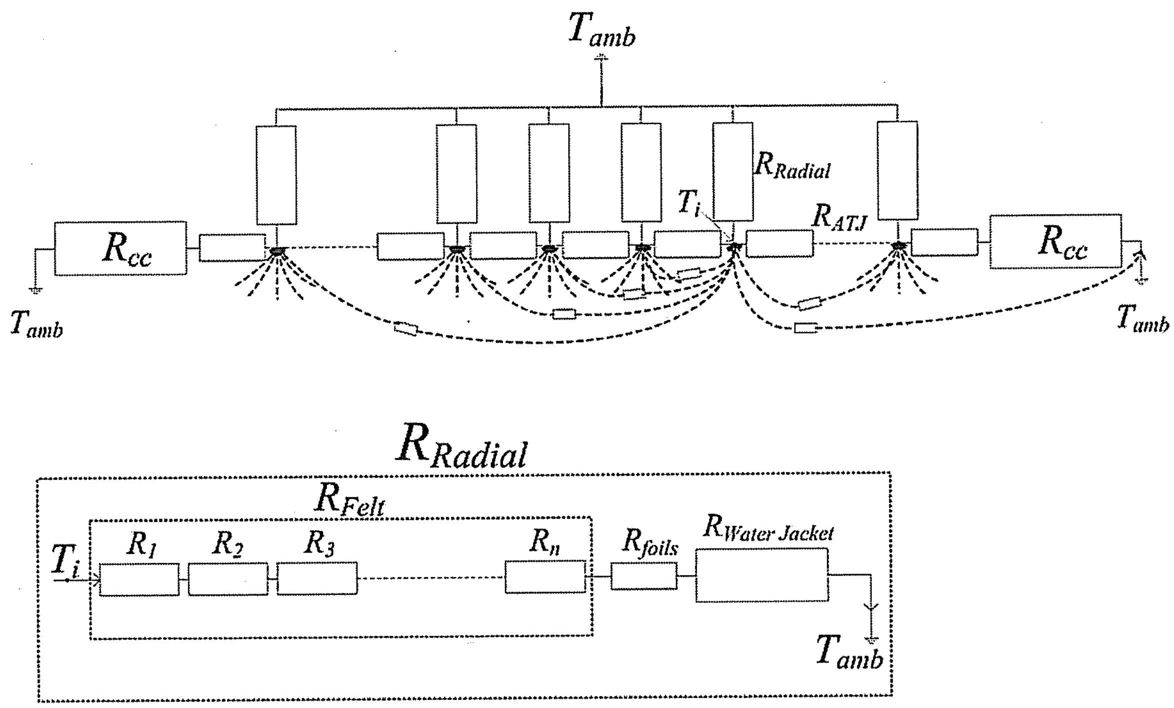

T_{amb}
R_{Radial}
T_i
R_{ATJ}
R_{cc}
R_{cc}
T_{amb}
T_{amb}
R_{Radial}
R_{Felt}
T_i
R_1
R_2
R_3
R_n
R_{foils}
$R_{Water\ Jacket}$
T_{amb}

Fig. 2

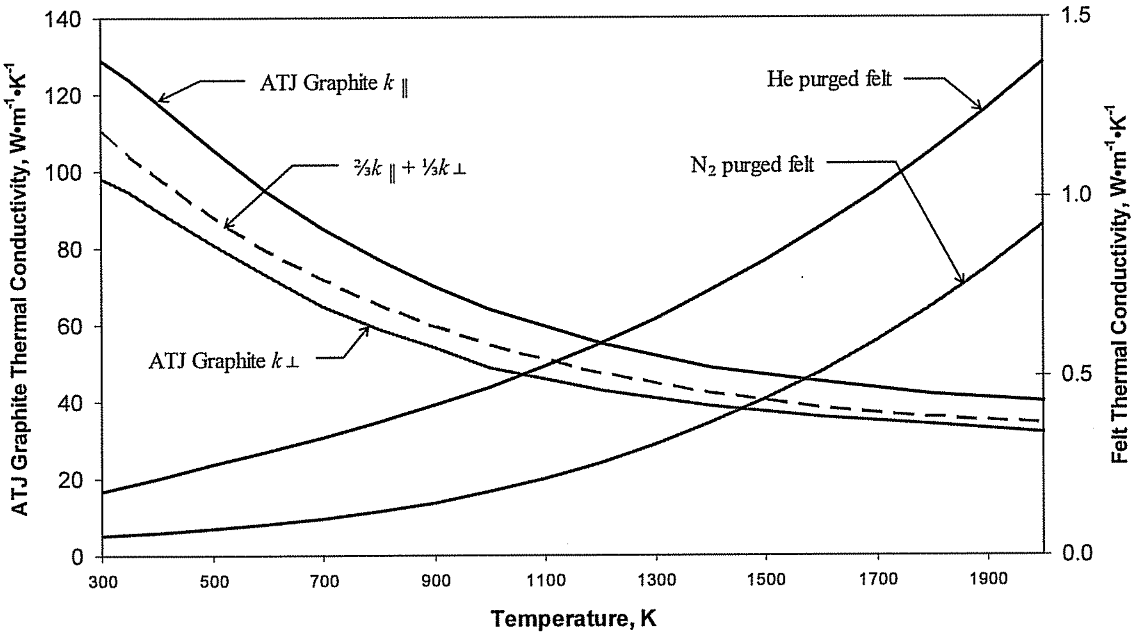

ATJ Graphite $k_\parallel$
$\frac{2}{3}k_\parallel + \frac{1}{3}k_\perp$
ATJ Graphite $k_\perp$
He purged felt
N_2 purged felt
ATJ Graphite Thermal Conductivity, $W \cdot m^{-1} \cdot K^{-1}$
Felt Thermal Conductivity, $W \cdot m^{-1} \cdot K^{-1}$
Temperature, K
140
120
100
80
60
40
20
0
1.5
1.0
0.5
0.0
300
500
700
900
1100
1300
1500
1700
1900

Fig. 3

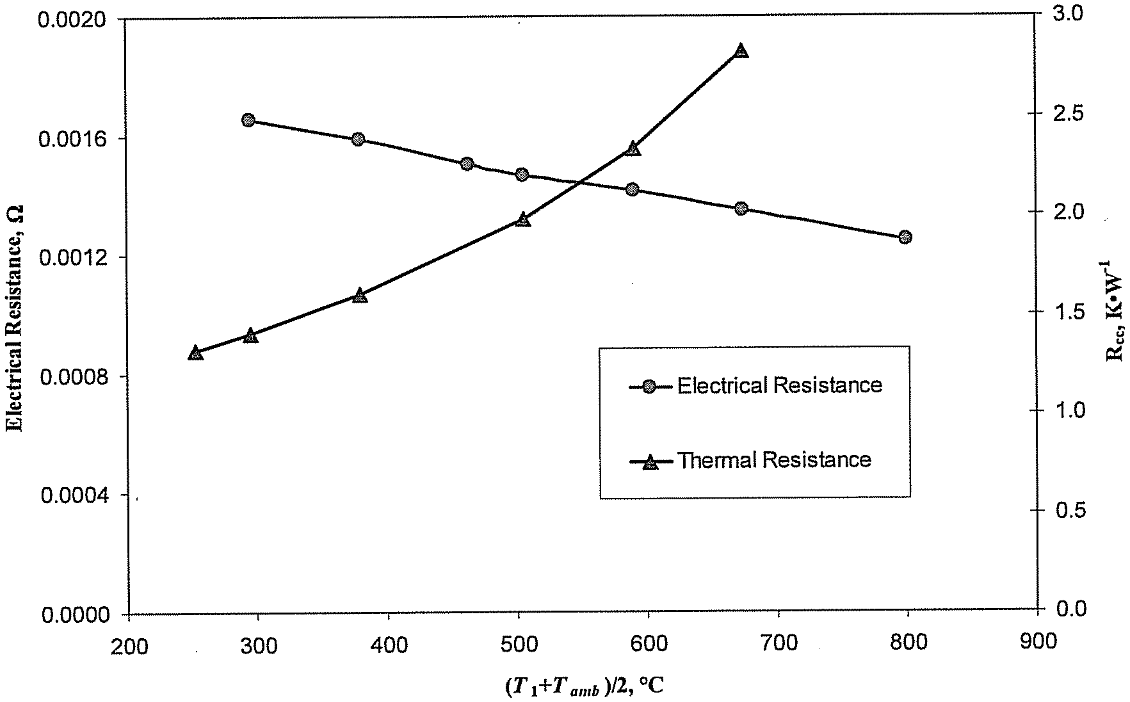
0.0020
0.0016
0.0012
0.0008
0.0004
0.0000
Electrical Resistance, Ω
3.0
2.5
2.0
1.5
1.0
0.5
0.0
R_{cc}, K•W^{-1}
Electrical Resistance
Thermal Resistance
200
300
400
500
600
700
800
900
$(T_1+T_{amb})/2$, °C

Fig. 4

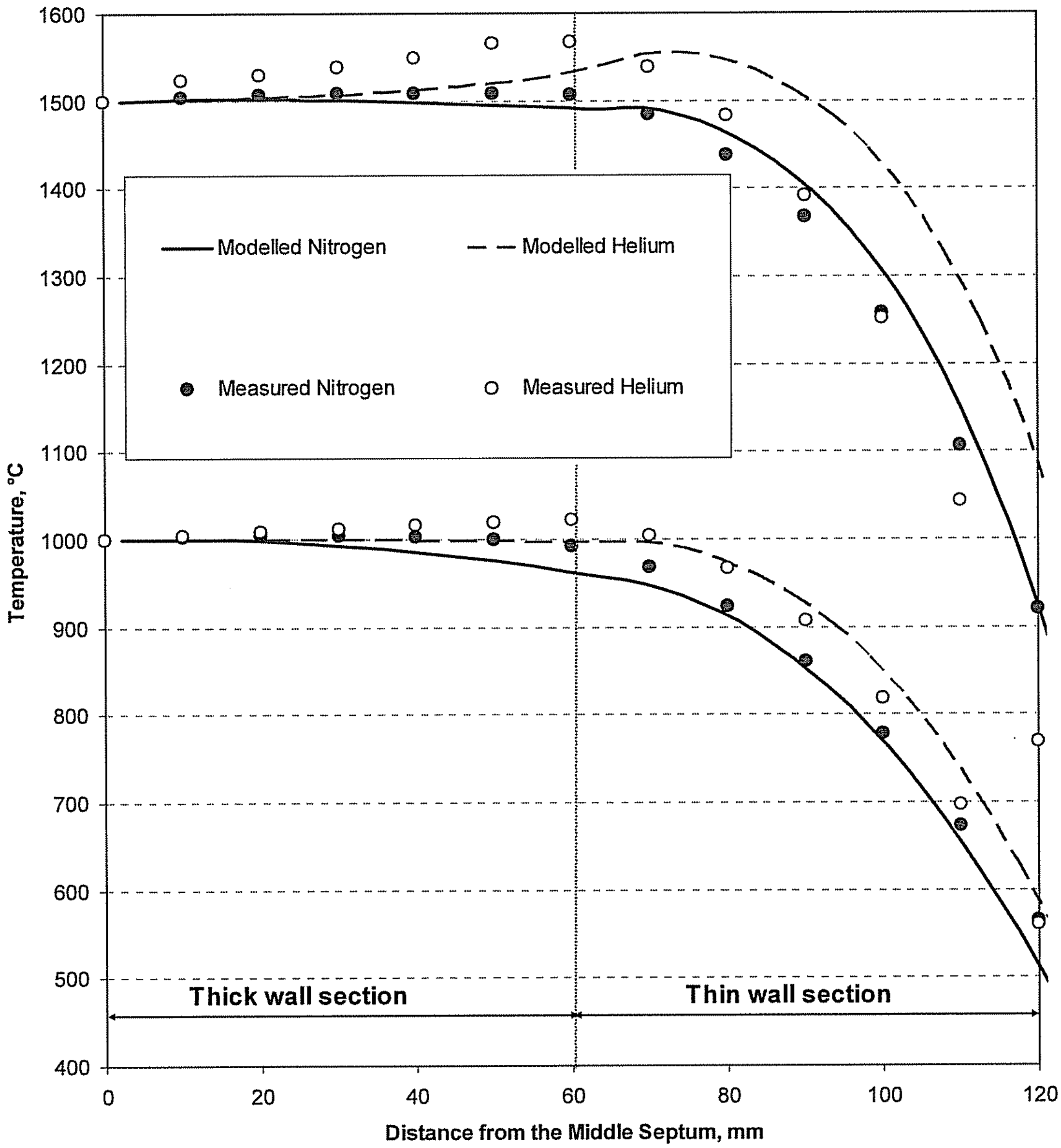

1600
1500
1400
1300
1200
1100
1000
900
800
700
600
500
400
Temperature, °C
Modelled Nitrogen
Modelled Helium
Measured Nitrogen
Measured Helium
Thick wall section
Thin wall section
0
20
40
60
80
100
120
Distance from the Middle Septum, mm

Fig. 5

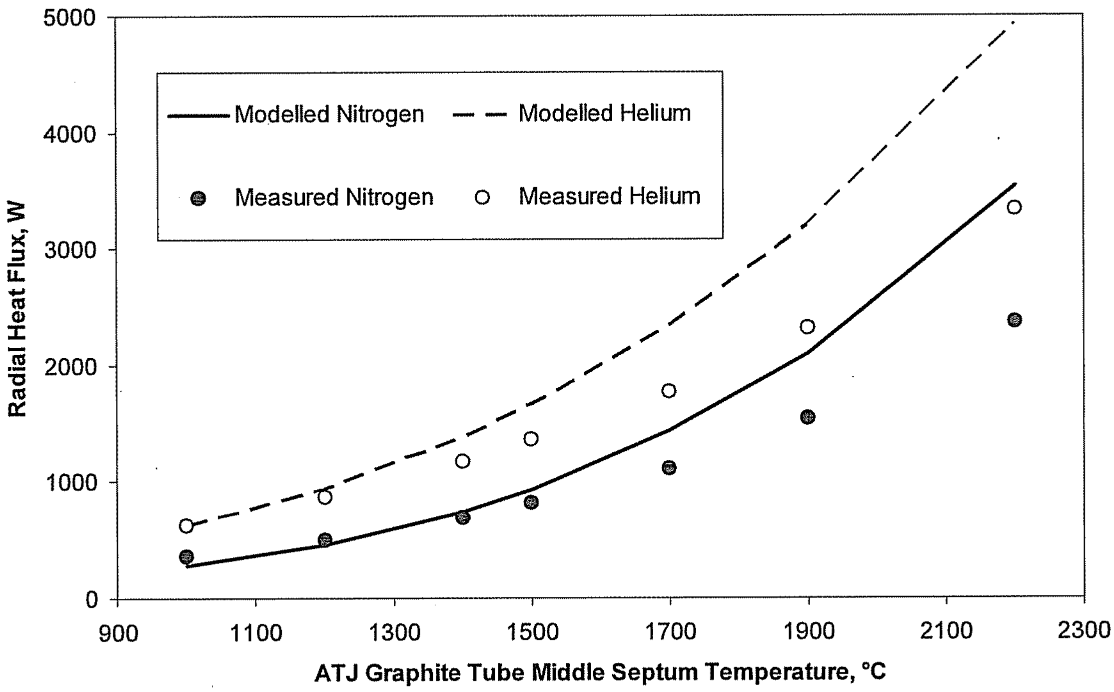

Modelled Nitrogen
Modelled Helium
Measured Nitrogen
Measured Helium
Radial Heat Flux, W
5000
4000
3000
2000
1000
0
900
1100
1300
1500
1700
1900
2100
2300
ATJ Graphite Tube Middle Septum Temperature, °C

Fig. 6

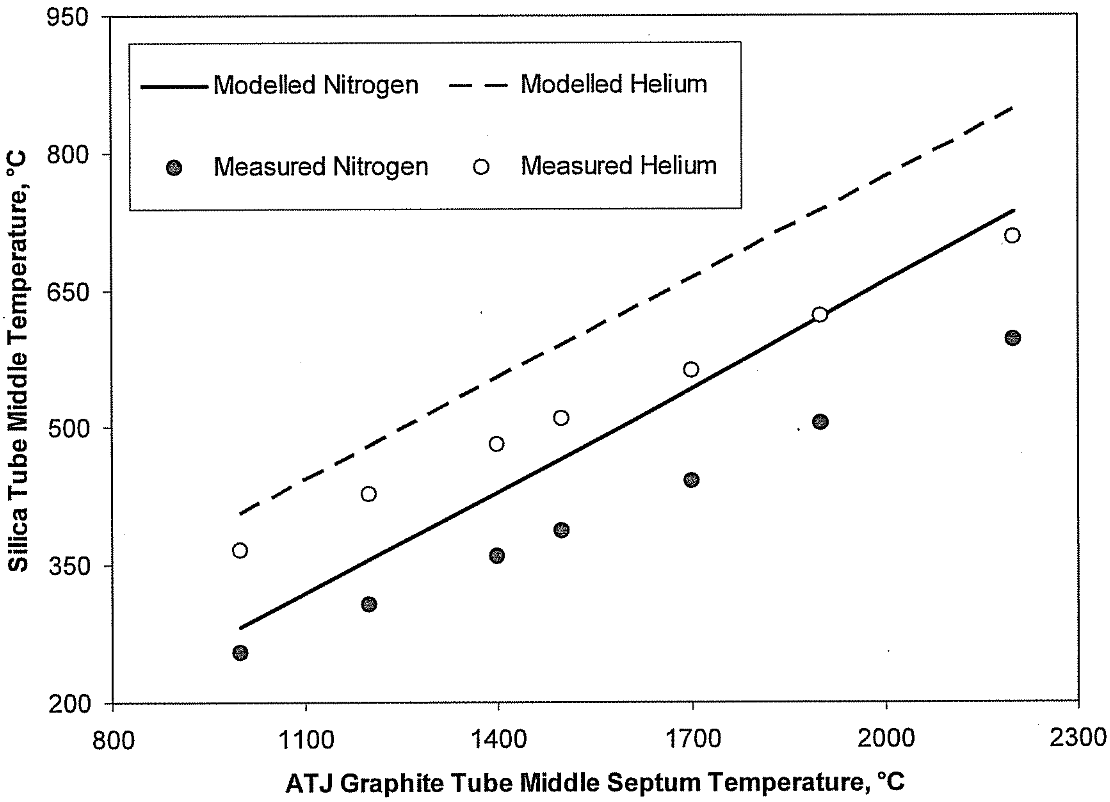
Modelled Nitrogen
Modelled Helium
Measured Nitrogen
Measured Helium
Silica Tube Middle Temperature, °C
950
800
650
500
350
200
800
1100
1400
1700
2000
2300
ATJ Graphite Tube Middle Septum Temperature, °C

Fig. 7